Available online at www.sciencedirect.com

Ceramics International 33 (2007) 1449–1453

CERAMICS INTERNATIONAL

www.elsevier.com/locate/ceramint

Preparation of $LiNiVO_4$ nano-powder using tartaric acid as a complexing agent

Titipun Thongtem *, Sulawan Kaowphong, Somchai Thongtem

Faculty of Science, Chiang Mai University, Chiang Mai 50200, Thailand

Received 13 February 2006; received in revised form 20 April 2006; accepted 21 May 2006

Abstract

$LiNiVO_4$ was prepared from Li_2CO_3, $Ni(CH_3COO)_2\cdot 4H_2O$ and NH_4VO_3 using tartaric acid as a complexing agent with 1:1–1:4 mole ratios of metals:tartaric acid and subsequent calcination at 350–700 °C for 6–12 h. Inverse spinel $LiNiVO_4$ was detected using XRD. FTIR and Raman analyses revealed the presence of stretching band of VO_4 tetrahedrons. Only Ni, V and O were detected by EDX. The 1:4 mole ratio for the product with 450 °C calcination for 6 h analyzed by SEM, TEM and electron diffraction (ED) composes of $LiNiVO_4$ nano-powder with 10–30 nm in diameter.

Keywords: Inverse spinel oxide; $LiNiVO_4$ nano-powder; Tartaric acid

---

1. Introduction

There are several kinds of transition metal oxides that can be used as cathode materials for lithium-ion batteries. They are $LiCoO_2$, $LiNiO_2$ and $LiMn_2O_4$ [1,2]. $LiCoO_2$ and $LiNiO_2$ are layered structure [2,3] but $LiMn_2O_4$ is normal spinel structure [3,4]. Following the discovery of these oxides, $LiNiVO_4$ has been found to be very attractive due to its inverse spinel structure [1,5,6]. It can offer a voltage as high as 4.8 V [7,8]. It is believed that preparation processes can play a role in the properties of electrode materials. Solid state reaction is a mechanochemical process but the product contains irregular morphology, larger crystallite size, non-stoichiometric phase, impurities and others [1,3,9]. Chemical solution processes have been found to be able to solve such the problems. Among them are starch-assisted combustion [1], citric complex method [10] and glycerol-assisted gel combustion route [9]. Only the product prepared by the last method was claimed to be nano-crystallite size. For the present research, $LiNiVO_4$ nano-powder was prepared by using polymerized complex method with tartaric acid as a complexing agent. The powder was purified by controlling mole ratio of total metals (M) to tartaric acid (TA) and by calcination at a variety of temperatures and times.

2. Experiment

By using tartaric acid as a complexing agent, Li_2CO_3, $Ni(CH_3COO)_2\cdot 4H_2O$ and NH_4VO_3 solutions were mixed and stirred to form carboxylate precursors (blue xerogel) which were subsequently calcined to form powder. The preparation is schematically shown in Fig. 1. The precursors and powder were intensively analyzed using XRD operated at 20 kV, 15 mA and a Cu Kα source, FTIR with KBr as a diluting agent and operated in the range 400–4000 cm^{-1}, Raman spectrometer using 30 mW He-Ne Laser with $\lambda = 632.8$ nm, SEM equipped with EDX operated at 15 kV and TEM as well as electron diffraction (ED) operated at 200 kV.

3. Results and discussion

3.1. XRD

Carboxylate precursors (M:TA = 1:1) with and without calcination at high temperature were analyzed using XRD and JCPDS standard [11]. The spectra are shown in Fig. 2. XRD spectrum of carboxylate precursors (A1) is broad showing that

---

* Corresponding author. Tel.: +66 53 943341/45; fax: +66 53 892277.
E-mail addresses: ttpthongtem@hotmail.com, ttpthongtem@yahoo.com (T. Thongtem).

0272-8842/$32.00 © 2006 Elsevier Ltd and Techna Group S.r.l. All rights reserved.
doi:10.1016/j.ceramint.2006.05.005

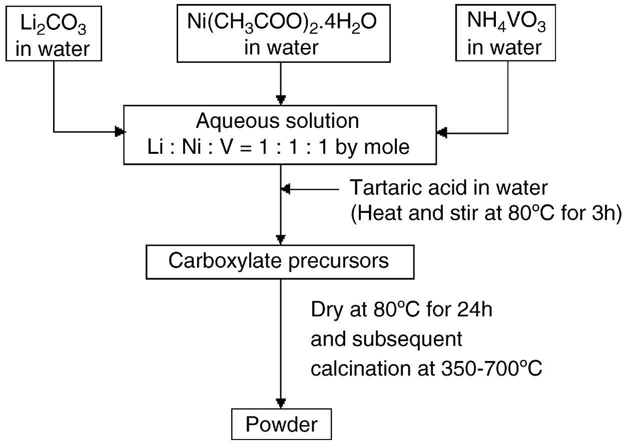

Fig. 1. Schematic diagram used for preparation of $LiNiVO_4$.

they are amorphous. At 350 °C calcination for 6 h (B), $LiNiVO_4$ with NiO, Li_3VO_4 and $LiVO_3$ impurities were detected showing that $LiNiVO_4$ started to form but its concentration is rather low. The degree of crystallinity is improved when the calcination temperature is further increased. This leads to the increase of XRD intensity. During increasing of the calcination temperature, the purity was also increased. For the calcination at 400 °C for 6 h (C), 450 °C for 6 h (D1) and 450 °C for 6 h with further calcination at 500 °C for 12 h (E1), $LiNiVO_4$ containing NiO impurity was detected. But for the calcination at 450 °C for 6 h and further calcination at 550–700 °C for 12 h (E2, E3, E4 and E5), a single phase of $LiNiVO_4$ was detected. XRD spectra show that the strongest peak is at $2\theta = 36.3°$ and diffracts from (3 1 1) plane. Two peaks at $2\theta = 30.8$ and $18.6°$ diffract from (2 2 0) and (1 1 1) planes, respectively. The first is much stronger than the second. This character is the specification of inverse spinel structure [4,8,12]. Oxidation states of cations in $LiNiVO_4$ are Li^{1+}, Ni^{2+} and V^{5+}. Octahedral interstices are equally and randomly occupied by Li^{1+} and Ni^{2+} but tetrahedral interstices are occupied by V^{5+} [4]. The $I_{(2\ 2\ 0)}/I_{(3\ 1\ 1)}$ intensity ratios are very close to 0.5 showing that the degree of crystallinity of $LiNiVO_4$ is very high [12].

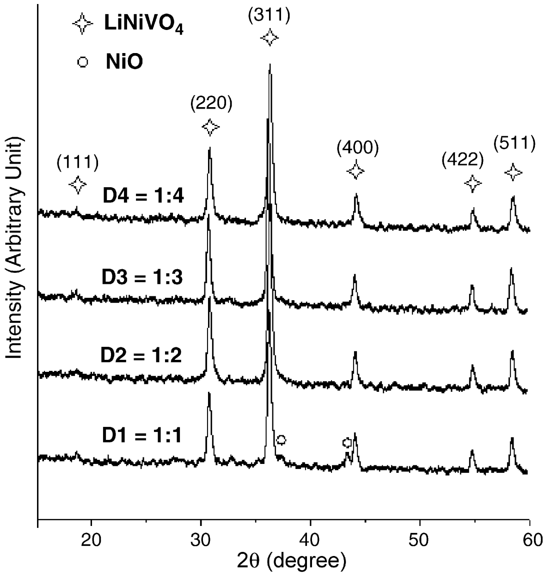

Fig. 3. XRD spectra of $LiNiVO_4$ (450 °C calcination for 6 h) for M:TA = 1:1, 1:2, 1:3 and 1:4.

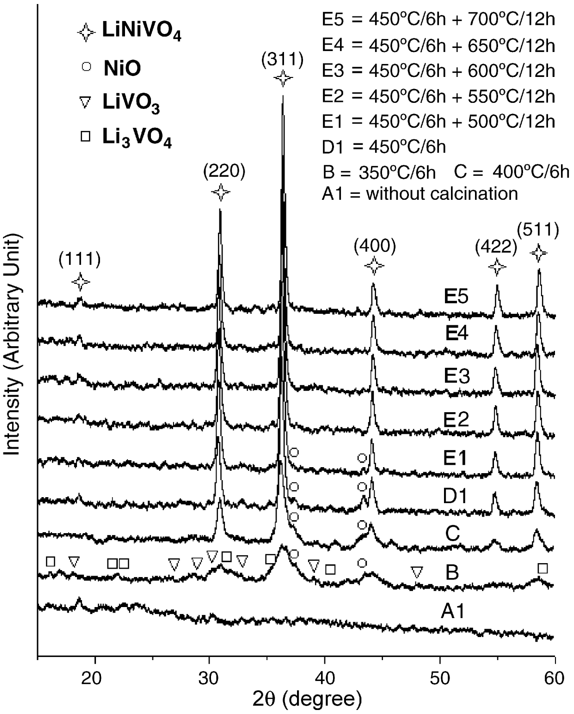

Fig. 2. XRD spectra of carboxylate precursors (M:TA = 1:1) with and without calcination at a variety of temperatures and times.

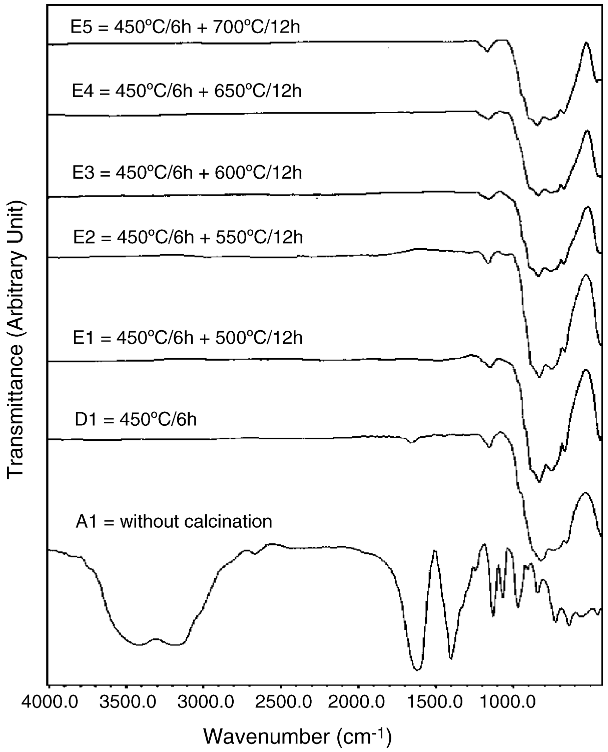

Fig. 4. FTIR spectra of carboxylate precursors (M:TA = 1:1) with and without calcination at a variety of temperatures and times.

Alternatively, $LiNiVO_4$ can be purified by using the excess acid. XRD spectra of the powder for a variety of M:TA mole ratios with 450 °C calcination for 6 h are shown in Fig. 3. For M:TA = 1:1 (D1), there was the detection of $LiNiVO_4$ with NiO impurity. The purity of $LiNiVO_4$ is increased with an increasing the amount of acid. For M:TA = 1:2 (D2), 1:3 (D3) and 1:4 (D4), single phase of $LiNiVO_4$ was detected. The excess acid is likely to assist in completing the complex formation.

3.2. FTIR

FTIR spectra of carboxylate precursors (M:TA = 1:1) with and without calcination at high temperature are shown in Fig. 4. The spectrum of carboxylate precursors (A1) shows that O–H stretching band of residual water and acid was detected at 2900–3700 cm^{-1} [13]. There were asymmetric and symmetric COO stretching bands of carboxylate group at 1604 and 1397 cm^{-1}, respectively [13]. When the precursors were calcined at high temperature (D1, E1, E2, E3, E4 and E5), all the residual water evaporated and O–H stretching band no longer exists. At 450 °C calcination for 6 h (D1), very small band of carboxylate groups was detected. When the temperature was further increased (E1, E2, E3, E4 and E5), the bands disappear showing that the carboxylate precursors were completely decomposed. The D1, E1, E2, E3, E4 and E5 spectra show that three splitting bands were detected at 634, 727 and 806 cm^{-1} specified as the stretching bands of VO_4 tetrahedrons [14]. They are the character of inverse spinel structure [14]. The splitting is likely to be from bonding of Li and Ni with O in VO_4 tetrahedrons [14,15]. In addition, two asymmetric stretching bands of NiO_6 octahedrons and of Li–O in LiO_6 environment were detected at 1126 [14,15] and 420 cm^{-1} [14,16], respectively.

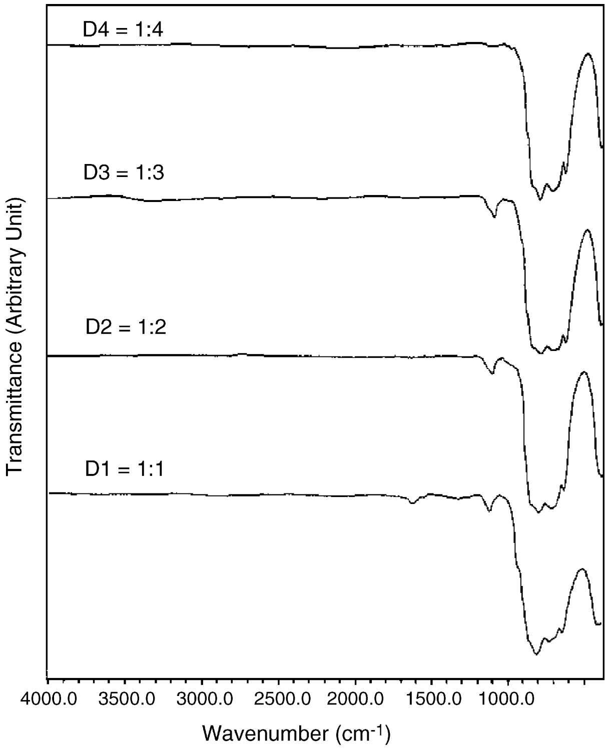

Fig. 5. FTIR spectra of $LiNiVO_4$ (450 °C calcination for 6 h) for M:TA = 1:1, 1:2, 1:3 and 1:4.

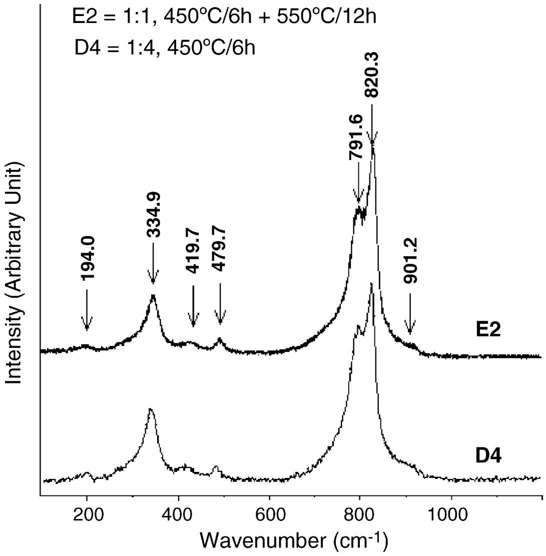

Fig. 6. Raman spectra of purified $LiNiVO_4$ for D4 and E2.

FTIR spectra of carboxylate precursors prepared by using a variety of M:TA mole ratios and subsequent calcination at 450 °C for 6 h are shown in Fig. 5. With the exception of M:TA = 1:4 (D4), asymmetric stretching band of NiO_6 octahedrons was detected at 1126 cm^{-1} [14,15]. The excess acid seems to play a role in the disappearance of NiO_6 octahedral band. In some cases, asymmetric stretching band of NiO_6 octahedrons was not detected [9,10].

3.3. Raman spectra

Raman spectra of purified $LiNiVO_4$ for D4 (M:TA = 1:4, 450 °C calcination for 6 h) and E2 (M:TA = 1:1, calcination at 450 °C for 6 h and further calcination at 550 °C for 12 h) are shown in Fig. 6. For cubic spinel structure, it is in possession of $Fd3m(O_h^7)$ symmetry [4,14,16]. Five modes being symmetrical

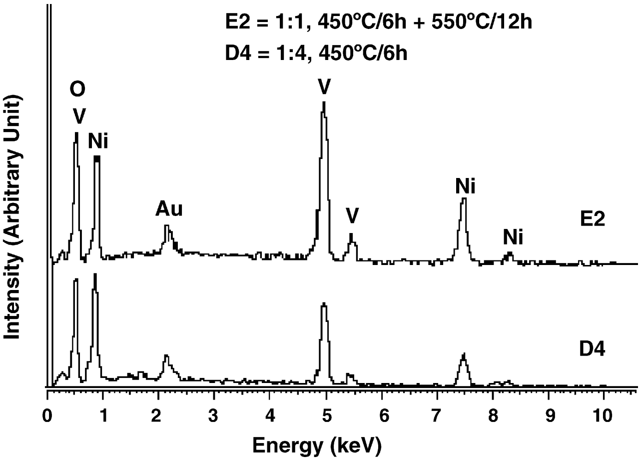

Fig. 7. EDX spectra of purified $LiNiVO_4$ for D4 and E2.

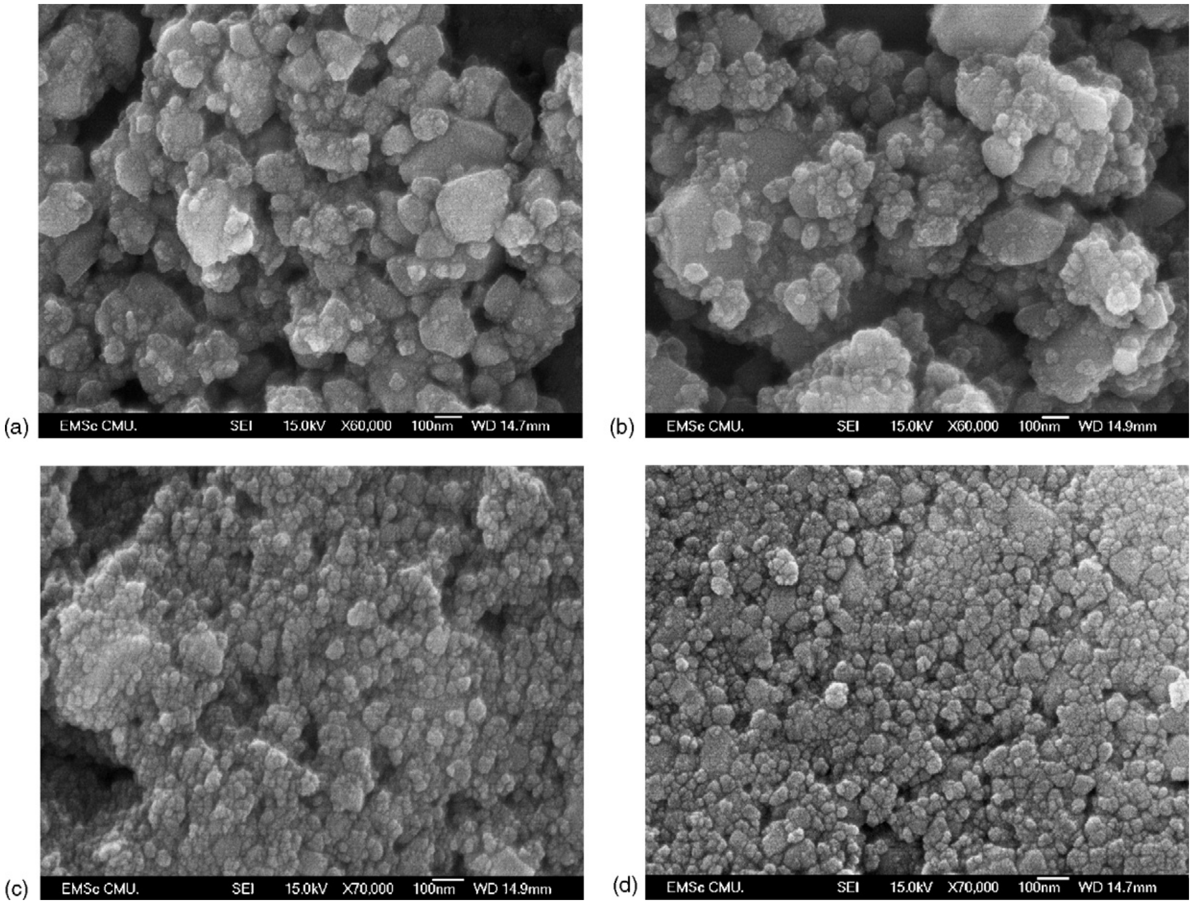

Fig. 8. SEM images of $LiNiVO_4$ (450 °C calcination for 6 h) at a variety of M:TA mole ratios: (a) 1:1, (b) 1:2, (c) 1:3 and (d) 1:4.

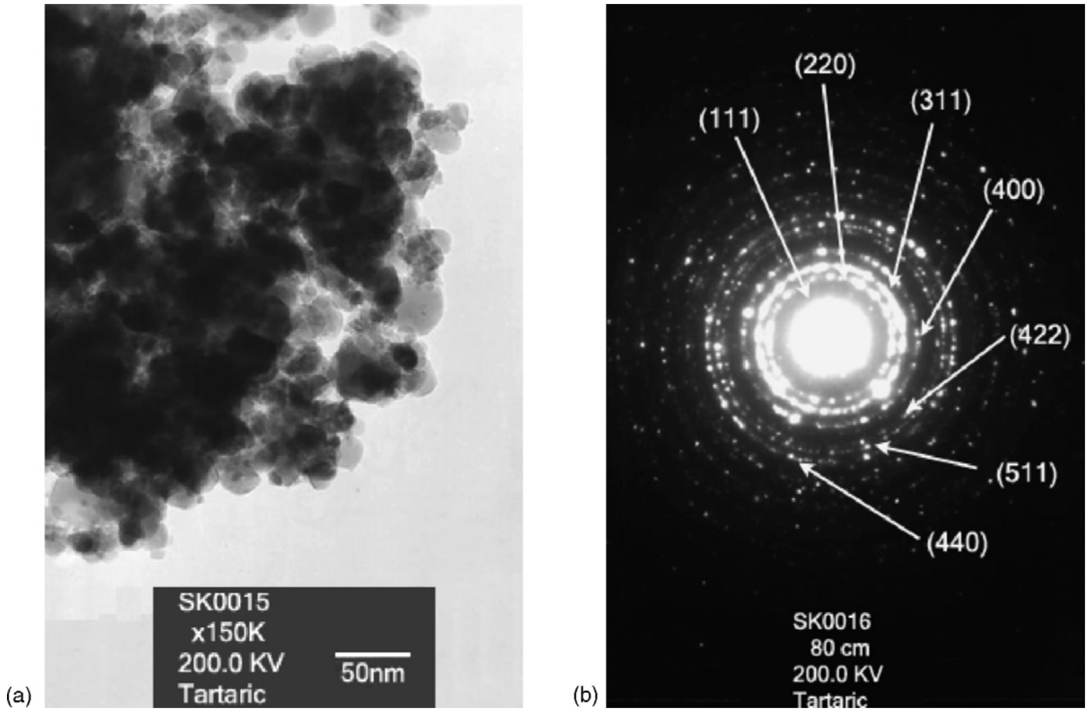

Fig. 9. (a) TEM image and (b) ED pattern of purified $LiNiVO_4$ for D4 (M:TA = 1:4, 450 °C calcination for 6 h).

with the inversion center ($A_{1g} + E_g + 3F_{2g}$) are Raman active [4,14,16]. A strong band was detected at 700–850 cm^{-1} which are the VO_4 tetrahedral stretching frequencies [4,14]. They are the vibrational modes of bonding between O and V^{5+} [14]. The 820.3 and 334.9 cm^{-1} are the stretching mode of VO_4 tetrahedrons with A_{1g} symmetry and the bending mode of VO_4 tetrahedrons with E_g symmetry, respectively [4,14,16]. The highest frequency band is broad due to asymmetric bonding of VO_4 tetrahedrons [4,14,16]. The 791.6 cm^{-1} vibration is very close to the stretching frequency of ideal VO_4 tetrahedrons [4]. In addition, two stretching bands of Li–O and Li–O–Ni were, respectively, detected at 419.7 and 479.7 cm^{-1} [4,16]. Comparing between Raman and FTIR spectra of E2, the asymmetric vibrational mode of NiO_6 octahedrons was detected only in the FTIR spectrum. The non-detection of asymmetric vibrational mode in Raman spectrum is due to the small change of polarization caused by Ni-O stretching vibration [15].

3.4. EDX

EDX spectra of purified $LiNiVO_4$ for D4 and E2 are shown in Fig. 7. At both calcination conditions, Ni, V and O were detected. Ni:V atomic ratios for both products are 1:1 which are in accord with the chemical formulae of $LiNiVO_4$. Li is the lightest metallic element and cannot be detected. To improve conductivity during the EDX analysis, Au was sputtered on top of the samples and was detected.

3.5. SEM

SEM images of $LiNiVO_4$ prepared by a variety of M:TA mole ratios and subsequent calcination at 450 °C for 6 h are shown in Fig. 8. Particle diameters are decreased with the increase of acidic concentration. At 1:1 (D1) and 1:2 (D2) mole ratios, the products compose of particles with different sizes and shapes which collect into agglomerations. But for higher acidic concentration at 1:3 (D3) and 1:4 (D4) mole ratios, the particles become rounder and are over the range of 10–30 nm in diameter. The agglomerations become smaller showing that round particles promote the segregation process.

3.6. TEM and ED

TEM image and ED pattern of purified $LiNiVO_4$ for D4 are shown in Fig. 9. It shows fluffy morphology due to the aggregation of small round particles. They are 10–30 nm in diameter which is in accord with the particle diameter analyzed by SEM. The ED pattern shows several concentric rings of bright spots with different intensities. The values of *d*-spacing corresponding to the diffraction planes of the nano-crystalline product were calculated [17] and compared with those of the JCPDS standard [11]. It was found that the diffraction rings correspond to (1 1 1), (2 2 0), (3 1 1), (4 0 0), (4 2 2), (5 1 1) and (4 4 0) planes of the product and that the diffraction pattern corresponds to $LiNiVO_4$. Intensity of (3 1 1) plane is at the highest.

4. Conclusions

$LiNiVO_4$ was successfully prepared by polymerized complex method using tartaric acid as a complexing agent. It can be purified either by high temperature calcination (E2, E3, E4 and E5) or by increasing the amount of acid at low temperature (D2, D3 and D4). Inverse spinel $LiNiVO_4$ was specified using XRD, FTIR, Raman, ED and EDX analyses. The 1:4 mole ratio for purified $LiNiVO_4$ with 450 °C calcination for 6 h (D4) analyzed by SEM and TEM composes of round particles with 10–30 nm in diameter.

Acknowledgement

We are grateful to the Commission on Higher Education, Bangkok Thailand, for funding the research.

References

[1] P. Kalyani, N. Kalaiselvi, N. Muniyandi, An innovative soft-chemistry approach to synthesize $LiNiVO_4$, Mater. Chem. Phys. 77 (2002) 662–668.
[2] G.T.K. Fey, K.S. Wang, S.M. Yang, New inverse spinel cathode materials for rechargeable lithium batteries, J. Power Sources 68 (1997) 159–165.
[3] H.W. Chan, J.G. Duh, S.R. Sheen, $LiMn_2O_4$ cathode doped with excess lithium and synthesized by co-precipitation for Li-ion batteries, J. Power Sources 115 (2003) 110–118.
[4] G.T.K. Fey, D.L. Huang, Synthesis, characterization and cell performance of inverse spinel electrode materials for lithium secondary batteries, Electrochim. Acta 45 (1999) 295–314.
[5] G.T.K. Fey, W.B. Perng, A new preparation method for a novel high voltage cathode material: $LiNiVO_4$, Mater. Chem. Phys. 47 (1997) 279–282.
[6] M.S. Bhuvaneswari, S. Selvasekarapandian, O. Kamishima, J. Kawamura, T. Hattori, Synthesis and structural analysis of lithium nickel vanadate, Mater. Chem. Phys. 91 (2005) 94–98.
[7] C.H. Lu, W.C. Lee, S.J. Liou, G.T.K. Fey, Hydrothermal synthesis of $LiNiVO_4$ cathode material for lithium ion batteries, J. Power Sources 81–82 (1999) 696–699.
[8] W. Chen, L.Q. Mai, Q. Xu, Q.Y. Zhu, H.P. Yang, Novel soft solution synthesis and characterization of submicromic $LiCoVO_4$, Mater. Sci. Eng. B 100 (2003) 221–224.
[9] S. Vivekanandhan, M. Venkateswarlu, N. Satyanarayana, Glycerol-assisted gel combustion synthesis of nano-crystalline $LiNiVO_4$ powders for secondary lithium batteries, Mater. Lett. 58 (2004) 1218–1222.
[10] J.R. Liu, M. Wang, X. Lin, D.C. Yin, W.D. Huang, Citric acid complex method of preparing inverse spinel $LiNiVO_4$ cathode material for lithium batteries, J. Power Sources 108 (2002) 113–116.
[11] Powder Diffraction File, JCPDS—International Centre for Diffraction Data, PA 19073-3273, USA, 2001.
[12] S. Chitra, P. Kalyani, B. Yebka, T. Mohan, E. Haro-Poniatowski, R. Gangadharan, C. Julien, Synthesis, characterization and electrochemical studies of $LiNiVO_4$ cathode material in rechargeable lithium batteries, Mater. Chem. Phys. 65 (2000) 32–37.
[13] B. Smith, Infrared Spectral Interpretation, CRC Press, New York, 1999.
[14] M.S. Bhuvaneswari, S. Selvasekarapandian, O. Kamishima, J. Kawamura, T. Hattori, Vibrational analysis of lithium nickel vanadate, J. Power Sources 139 (2005) 279–283.
[15] Q.Y. Lai, J.Z. Lu, X.L. Liang, F.Y. Yan, X.Y. Ji, Synthesis and electrochemical characteristics of Li-Ni vanadates as positive materials, Int. J. Inorganic Mater. 3 (2001) 381–385.
[16] S.R.S. Prabaharan, M.S. Michael, S. Radhakrishna, C. Julien, Novel low-temperature synthesis and characterization of $LiNiVO_4$ for high-voltage Li ion batteries, J. Mater. Chem. 7 (1997) 1791–1796.
[17] K.W. Andrews, D.J. Dyson, S.R. Keown, Interpretation of Electron Diffraction Patterns, Plenum Press, New York, 1971.